

UNCLASSIFIED

## Defense Technical Information Center Compilation Part Notice

ADP010528

TITLE: Rapid Aerodynamic Data Generation using an  
Iterative Approximation Method

DISTRIBUTION: Approved for public release, distribution unlimited

This paper is part of the following report:

TITLE: Aerodynamic Design and Optimisation of  
Flight Vehicles in a Concurrent  
Multi-Disciplinary Environment [la Conception et  
l'optimisation aerodynamiques des vehicules  
aeriens dans un environnement pluridisciplinaire  
et simultane]

To order the complete compilation report, use: ADA388284

The component part is provided here to allow users access to individually authored sections of proceedings, annals, symposia, ect. However, the component should be considered within the context of the overall compilation report and not as a stand-alone technical report.

The following component part numbers comprise the compilation report:

ADP010499 thru ADP010530

UNCLASSIFIED

## Rapid Aerodynamic Data Generation using an Iterative Approximation Method.

C. A. Toomer

British Aerospace Sowerby Research Centre,  
CFD Group, Mathematical Modelling Department,  
FPC 267, PO Box 5, Filton, Bristol,  
United Kingdom BS34 7QW

### Nomenclature

a	Coefficient used in function fitting expression
c	Chord length
CFD	Computational Fluid Dynamics
$C_D$	Coefficient of drag
$C_L$	Coefficient of lift
$C_M$	Pitching moment (y-direction)
Cp	Coefficient of pressure
M	Mach number
MDO	Multi-disciplinary Design Optimisation
PosMaxT	Position of Maximum thickness design variable
t	Parametric variable
x	Axial co-ordinate
y	Normal co-ordinate
z	Vertical co-ordinate
$\alpha$	Angle of attack (degrees)
$\beta$	Design variable (shape or operating condition)

### Subscripts

$\infty$	Freestream conditions
----------	-----------------------

### Introduction

Aerodynamic design and optimisation is a costly and complicated process in which numerically generated information about the design space plays a vital role. Hence the information needs to be of good quality, i.e. describing the correct physics, and to be easily accessible from databases using standardised formats. To make this process affordable and efficient, the codes must be fast, robust and accurate. Aerodynamic design problems tend to involve a large number of design parameters and constraints on the design. Large data sets are generated and so it is wise to automate the data generating and processing whenever possible.

Data generation is only part of the process. Efficient algorithms to access and interpret the data are required, as is an efficient means of negotiating through the design space. Optimisation is the usual method by which the data are analysed, and regions within the design space identified as possible design solutions or improvements to existing designs.

One of the aims of the work presented here is to use approximation methods to resolve functions of interest, through the use of simpler or easier to compute functions. These computed functions depend on the variables chosen in the parameterisation of the vehicle shape and the conditions at which it flies. The functions of interest are those describing the vehicle's performance, e.g. coefficients of lift, drag and pitching moment. The modelling enables the designer to learn about the relations between the design parameters and their effects on the vehicle performance. It is important to understand: the trade-offs between the accuracy of the model and the complexity of the function, and the amount of data & time required to achieve a useful description of the design space.

Another aim is to create frameworks of methods that allow the designer to easily and quickly enhance and modify the problem as knowledge is built up. For example, having run an optimisation case the designer may wish to amend the existing constraints or to add into the problem constraints on new quantities.

The Sowerby Research Centre of British Aerospace has a number of computational tools available for use in the conceptual design phase of a vehicle. Some are developed in-house, others obtained from outside, some tools are mature, others in development. For many of these programs physical accuracy is the prime concern, e.g. Navier-Stokes/Euler finite volume codes. Others are developed where it is felt that some accuracy can be sacrificed for substantial reductions in the time to identify viable solutions to the problem considered.

In this second category of codes are a forward design perturbation code (developed in-house) based on sensitivity analysis, and response surface methods. When combined in a multi-level optimisation strategy, reductions of between 70% to 95% have been obtained in the computational time required to find one or more solutions, compared with using a Computational Fluid Dynamics (CFD) code to produce the required aerodynamic data. The design variables used are both operating condition parameters (angle of attack and freestream Mach number) and geometric parameters (B-splines, bezier curves or "super-variables" for each aerofoil section: camber, thickness, position of maximum thickness and twist angle etc).

This paper is structured into three main sections. In the first section the routes chosen to obtain an improved design are discussed. In the second section are described the complementary methods used to parameterise the vehicle shape, generate the data describing its performance and to interpret this data for design problems. The third and final section details the conditions imposed in a design improvement study and

some of the results obtained. A generic wing-body is used as the testcase. Both single-point and multi-point results are shown. Multi-point analyses are extremely valuable in assessing the off-design performance of the vehicle. Modifying a design through single point optimisation may produce a configuration that is very sensitive to changes in design parameters.

The work presented here is the first stage of a two-part design improvement study. Only the results from the first stage are reported in this paper. The second stage, in which the viscous flow around the vehicle is studied, involves the predictions from the first stage, in particular the region of design space to be investigated. For configurations with regions of separated flow, the inviscid and viscous optimisation results may not indicate the same region of design space.

### **Routes to Design Improvement**

There is no route that consistently provides the best solution for all types of aerodynamic design optimisation problems. Both sequential approximate programming and direct insertion approaches are commonly used. In order to make these standard approaches more cost-effective; approximation techniques are included in the sequences used here. The codes linked together include a surface and field grid generator, a CFD code, a sensitivity code, curve fitting techniques and an optimiser.

Four approaches have been compared. Approaches 1 & 2 are sequential approximate programming approaches where the maximum benefits of approximations are used to speed up the time to find an improved design. Approaches 3 & 4 use a direct insertion approach, where the use of approximate data is limited and hence the accuracy of the data used by the optimiser is better than in approaches 1 & 2.

#### **Approach 1.**

The design space is chosen by setting, for each design variable, the range over which it can vary. A representative sample of points is chosen to model this design space, and at each point the CFD code is run to produce forces and moments data. The results are function fitted using polynomials, so that a mathematical representation exists for each force & moment coefficient as a function of the perturbed design variables. By partially differentiating these expressions, the first and second order gradients can be obtained. The expressions for the forces & moments and their sensitivities provide the optimiser with sufficient information at any point in the design space to perform its search for the minimum of the objective function.

#### **Approach 2.**

Approach 2 follows that of 1 except that the perturbation code is used to generate some of the data in place of the CFD code. This reduces the time required to find potential design configurations that satisfy the constraints in the optimisation problem. The CFD code is always used to evaluate information at the initial design point. All data required at points reasonably close to the initial design point are generated using the perturbation code. The tiered CFD/perturbation/function-fitting approach has been successfully used to improve aerofoil shape design for cruise conditions. The reduction in time of approach 2 compared with approach 1 can be up to 90% ([1]).

#### **Approach 3.**

Approach 3 is a direct insertion approach where the optimiser directs the path taken through the design space to find the minimum of the objective function. At each design point selected, data are evaluated by the CFD code to give the values of the objective and constraints and their sensitivities for each design parameter. The gradients are created by forward differencing. No response surface fits are used. The advantage with the method is that all data are as accurate as the CFD code can produce and so the optimiser follows a search path based on accurate information. There are disadvantages too. Care must be taken with the production of the gradients, in that reasonable step sizes must be used. Inaccurate gradients are produced using too large a stepsize, and also by using very small step-sizes since the gradient calculation is influenced by rounding errors and any cycling in the CFD solution. Substantial time is required by approach 3 to generate the required data as each design parameter must be perturbed to evaluate the gradient and that involves multiple runs of the CFD code at each design point considered. Finally information may be required at a design point for which the surface and/or volume grid poses problems for the flow code. In the case of the latter problem arising, an alternative design point, close to the specified point, must be used for which the analysis codes are successful, or the optimisation must be taken from a different initial point.

#### **Approach 4.**

Substantial savings in time can be made on approach 3 if the gradient calculation is performed by the perturbation code. Approach 4 uses the perturbation code not just for the gradient calculation but also when the new point chosen by the optimiser is reasonably near to the previous point. In that case the perturbation code is instructed to march to this point. In tests conducted by van Etten [2] using a line search with small steps, this approach can reduce the time required to find the minimum by 60-90% over approach 3.

#### **Convergence of the design search**

For all approaches except approach 3, the solution obtained by the optimiser is based on approximation data. Therefore the CFD code must be run at the design point proposed by the optimiser so as to provide the accurate values for the forces and moments. If the solution does not satisfy the problem within required design and accuracy limits, the approach is repeated.

In approaches 1 & 2, whenever a new design space is chosen or an existing one modified or sub-divided, sufficient data are evaluated to the limits of each new design space for the function fits. A new polynomial fit is found for each quantity modelled. New smaller design spaces are often constructed around solutions suggested by the optimiser, with this point at the centre of the new design space. The changes to the design space must make the functions described more accurate and relevant without excluding possible solutions. The optimisation is started using the new formulae and the sequence is continued until the agreed accuracy is met.

### **Parameterisation and Design Tools**

#### **Surface parameterisation and grid generation**

Many different parameterisations can be adopted to perform shape variation on vehicle configurations. In this case the parameterisation is that developed for the European Consortium MDO wing-body test case [3]. This generic civil aircraft has a wingspan of 80m, a take-off weight of 550 tonnes and seats 650 passengers. The

planform of the aircraft is kept constant during these design studies and only the sectional shape of the wing is allowed to vary. The wing is constructed from five aerofoil sections: at the root, crank, tip and intermediate (in-board and out-board) positions (see Figure 1).

The formulation ensures specific set values in each section for trailing edge angles, and the curvature of the nose, crest and trough. Other rules are applied to preserve the planform area, aspect ratio, sweep and dihedral. Hence there is limited opportunity for greatly altering the shape.

Each aerofoil is constructed in  $(x, z)$  space from four Bezier curves of fifth-order using the general formulation:

$$x(t) = x_0 - 5t(x_0 - x_1) + 10t^2(x_0 - 2x_1 + x_2) - 10t^3(x_0 - 3x_1 + 3x_2 - x_3) + 5t^4(x_0 - 4x_1 + 6x_2 - 4x_3 + x_4) - t^5(x_0 - 5x_1 + 10x_2 - 10x_3 + 5x_4 - x_5)$$

A similar formulation for the  $z$  co-ordinate is used.  $t$  is a parametric variable and the  $(x_n, z_n)$  are Bezier curve vertices for  $n=0, \dots, 5$ .

Two curves are on the upper surface of the aerofoil, two on the lower surface. For each surface, one curve extends from the leading edge to the crest (on the upper surface) or trough (on the lower surface). The other curve from the crest or trough to the trailing edge. In Figure 2 the four curves for the crank section of the wing in its default configuration, with the associated Bezier curve control points are shown.

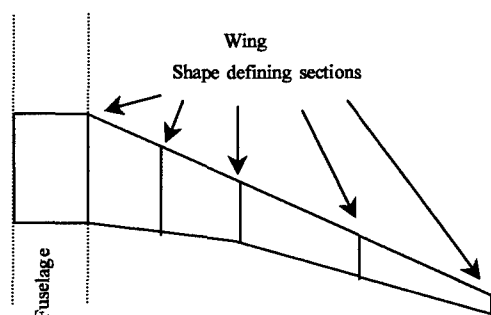


Figure 1: Schematic of the model geometry

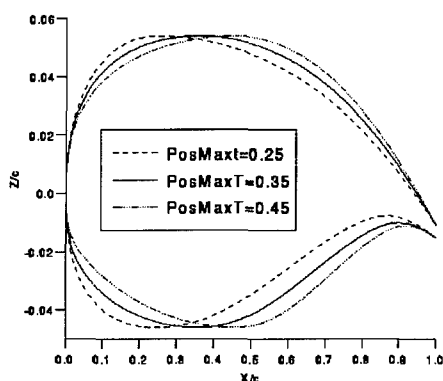


Figure 3 Effect on the aerofoil shape of varying the Position of maximum thickness parameter, PosMaxT

The user or the optimiser influences the shape of the aerofoil through assigning values to "super-variables": camber, twist, maximum thickness and position of maximum thickness for each aerofoil section. These values are used to evaluate the Bezier vertices. The aerofoil lengths are non-dimensionalised by the chord length,  $c$ . The position of maximum thickness variable, PosMaxT, controls the chordwise position of the trough and crest (Figure 3). These are located at the same  $z$ -coordinate value. Camber is restricted such that it affects only the rear portion of the aerofoil. An increase in camber causes the trailing edge to move downwards (Figure 4), and the trailing edge tangents to be rotated. The formula used is:

$$z(\text{tail}) = z(\text{tail\_orig}) - \text{camber}(1 - \text{PosMaxT})^2$$

Once the aerofoils are created they are positioned on the wing planform. Each aerofoil is rotated to the specified twist angle, and then the aerofoil is scaled to obtain the correct chord on the three-dimensional planform. Finally the aerofoils are placed on the 3D planform by applying dihedral, deriving the wing twist axis at quarter chord and positioning the aerofoil chordline to intersect with this reference axis.

After the wing is constructed, a surface mesh is produced and the multi-block field mesh extended from this. As structured meshes are used throughout this study, it is necessary to maintain the same number of blocks, and cells within each block, as in the original mesh.

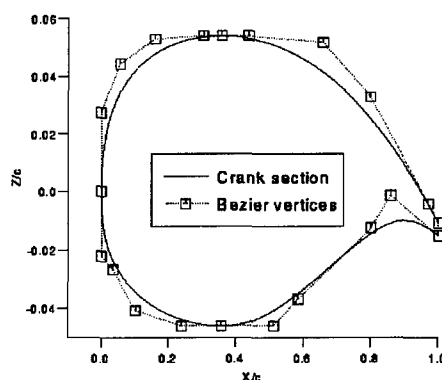


Figure 2. A parameterised wing section using Bezier curves. The position of the Bezier vertices is also plotted.

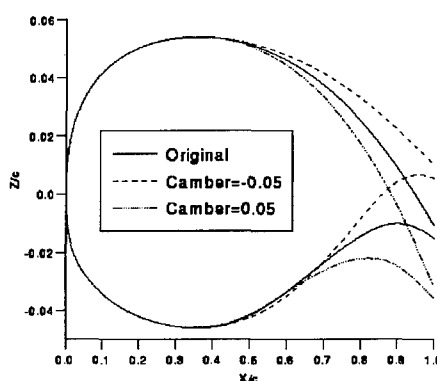


Figure 4 Effect on the rear aerofoil shape of varying the camber parameter from its original value of zero.

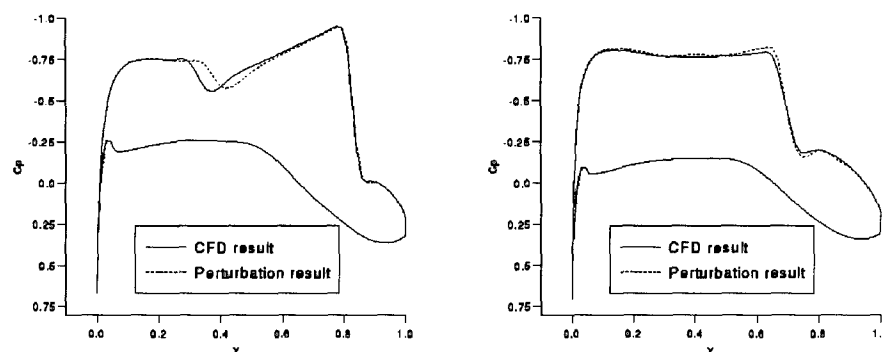


Figure 8. Comparison between the CFD and the perturbation surface  $C_p$  distributions at 41% and 74% chord respectively for the shape variation in the MDO wing. The results are sectional cuts of the  $C_p$  distributions in Figure 5. The  $x$  values have been scaled by the chord length.

The perturbation code produces flowfield predictions as well as forces and moments. The pressure coefficient distribution on the wing-body and on the symmetry plane at the final point of (0.35, 0.43, 0.44, 0.44, 0.42). is shown in Figure 5, as is the corresponding CFD solution on the final geometry. The same range and number of contours are used in both diagrams.

The range of values for  $C_p$ , [-1.044, 1.122] is predicted extremely well by the perturbation code. The only differences between the CFD and perturbation predictions occur on the upper wing surface in the vicinity of the shock, where the latter code has a tendency to smear a shock.

This effect can be shown better by taking sectional cuts through the wing. Comparison between the CFD and perturbation predictions for the surface  $C_p$  distributions at 41% and 74% chord are given in Figure 8. The upper surface distribution is not accurate in the mid-section of the wing where there is a small shock. The perturbation code prediction for this shock is in error by 1-2 cells in the 41% chord diagram. The position of the shock and the number of grid cells used to capture it are the predominant source of error in the perturbation results. However as shown by Figure 7, the error is not large enough to significantly affect the forces and moments data. It will be shown in the next section that the errors in the shock region do not deter from the code's usefulness in design improvement problems.

The methods used in the perturbation code may be applicable to other sets of nonlinear equations that describe well-behaved, continuous functions, e.g. forces and moment coefficients. Work is currently underway to evaluate the approach using nonlinear equations in structural modelling problems.

#### Function-fitting

There is a wealth of possible functions that can be used to model the available data. Aerodynamic forces and moments data tends to be smooth and continuous with few turning points per variable, even though there are discontinuities (shocks) present in the transonic flow around the vehicle. The function fits utilised in these cases involve those with and those without cross terms. For expressions with cross terms, the data are targeted toward more specific regions that are known to be of interest.

In these examples the shape design parameters are themselves functions of other variables (i.e. the Bezier vertices). Hence the parameters are not necessarily independent of each other. Function fitting using the

summation of separate expressions for each design variable may miss any inter-dependence. The use of cross-terms in the function fitting, and using data in which more than one parameter has been varied, can be used to establish the inter-dependence of the parameters.

The expression used without cross terms involves a three-level star design: a central point, points near the centre, and points toward the design boundary. A fourth order polynomial is used for each parameter perturbed, and these polynomials are summed to give the coefficient expression. The advantage with this type of expression is that as the number of design parameters is increased, the number of data points required to model the extended function increases linearly. The accuracy does not degrade with an increase in design parameters as long as care is taken not to make the parameter ranges too large.

The disadvantages with this type of modelling is the small number of points used to describe the response due to each parameter and the lack of information on parameter interactions due to no cross-terms.

The drag coefficient can be represented as:

$$C_D = a_0 + \sum_{j=1}^{NTOT} \sum_{n=1}^4 a_{nj} \beta_j^n$$

where NTOT is the number of design variables,  $\beta_j$  are the design variables,  $a_0, a_{nj}$  are the polynomial coefficients whose values are found from function fitting the data. Similar expressions are used for the other functions (e.g. lift coefficient, pitching moment, surface Mach number) with different values for the coefficients. The response surfaces for the lift and drag coefficients (in one of the typical design spaces considered in this study), showing the variation with crank and tip camber (all other design variables kept to those of the reference position) are shown in Figure 9.

Expressions with cross-terms can be computationally more complex in requiring far larger amounts of data to fit, but they are not more complex in terms of the design parameters being modelled. The data are initially selected from the simpler no cross-term data, with additional points generated within regions of the domain known to be of interest where more than one parameter varies from the values at the initial/central point. The advantage is that parameter interactions are considered in the modelling. The disadvantages with this type of function are the time to generate the required data, and

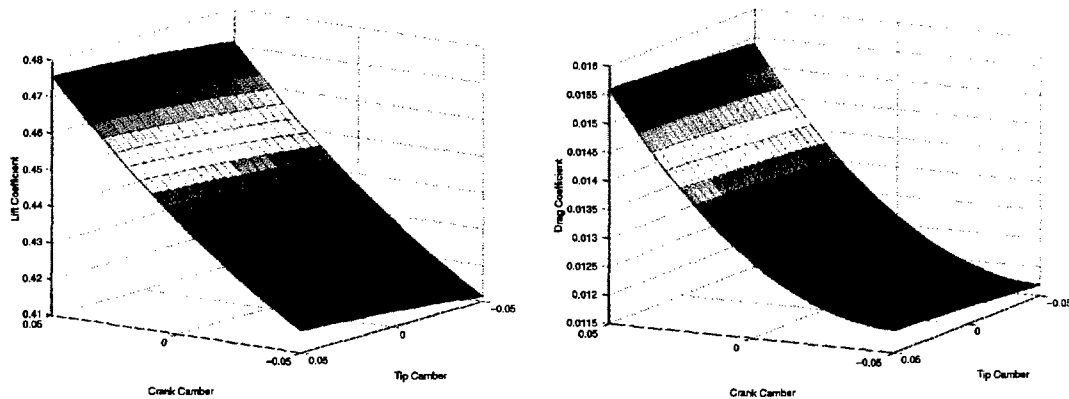


Figure 9 Function fitted data for the lift and drag coefficients on the wing using a quadratic expression with cross-terms. The crank and tip cambers are allowed to vary. All other parameter values are set to those at the reference point in design space.

deciding which points are good representatives of the design space. This problem increases as the number of design parameters increase. The cross term function used in this study uses a summation of linear and quadratic terms.

$$C_D = a_0 + \sum_{j=1}^{NTOT} a_j \beta_j + \sum_{j=1}^{NTOT} a_{jj} \beta_j^2 + \sum_{1 \leq j < k \leq NTOT} a_{jk} \beta_j \beta_k$$

With NTOT design variables the quadratic expression requires

$$\frac{1}{2}(NTOT + 1)(NTOT + 2)$$

data points. Hence for the 20 shape variables and the angle of attack, 253 data points are required.

The values from the functions generally compare well with the corresponding values obtained from the CFD code for small design spaces. However it is important to work within the design space defined by the function fitted data. As the amount of data describing a domain increases, the domain can be sub-divided and function fits of the data within each sub-domain can be used. The drawback with this approach is that at the boundary between sub-domains, the gradients of objective and constraint functions may be different in each region. The large domain space also needs to be shrunk to a number of smaller, isolated, sub-domains, each modelling the design space around a potentially favourable design solution.

Function fits substantially simplify the application to optimisation studies where the objective and constraint functions consist of these explicit mathematical expressions from which the partial derivatives are readily available. The optimisation strategy permits the design space size to be amended and/or additional constraints to be quickly added to the problem, through utilisation of the data stored when using the CFD and perturbation codes. These situations occur when either the designer wishes to test the solutions to the optimisation problem and evaluate which designs are most suitable, or when the designer wishes to pose a slightly different optimisation problem to the same design space. A further advantage with using function fits is that estimates of the quantities needed by the optimiser are available for any point in the design space, and the search does not stop due to problems obtaining surface or volume geometries at specified design points.

The disadvantages to be overcome with function fitting: the accuracy depends on the function model and on the choice of experimental design. Large inaccuracies can arise if the range over which a design parameter is being modelled is large and/or if a parameter is highly sensitive.

#### The Optimisation Routine

The optimisation algorithm used is a sequential quadratic programming algorithm from the NAG Fortran library [6]. The search direction is the solution of a quadratic programming problem. Since a gradient-based optimiser is effective in searching for a local minimum, in all the experiments described here, runs are performed at different initial design points. This increases the chance that the optimiser will consider design points in different regions. The larger the number of design variables, the more test cases need to be performed.

#### Design Improvement Studies

##### Test case considered

In the following optimisation problems, the MDO aircraft is assumed to be flying at cruise conditions of  $M_\infty 0.85$ . The CFD and sensitivity codes are run for steady state inviscid flow only. The design parameters permitted to vary are the angle of attack and for each aerofoil section: the camber and the twist. In some cases the position of maximum thickness varies too. The chosen starting point has  $\alpha=0.5$  degrees, zero camber and the twist and position of maximum thickness vectors are:

$$(2.364, 1.286, 0.155, -0.684, -1.638), \\ (0.287, 0.350, 0.358, 0.358, 0.341)$$

respectively. The thickness for each aerofoil section is kept to the original values of:

$$(0.14, 0.12, 0.10, 0.094, 0.088)$$

The design space is set to  $[-0.01, 0.05]$  for each cambered section,  $[-7, 5]$  degrees for the twist angles,  $[0.25, 0.45]$  for the positions of maximum thickness and  $[-1.5, 2.5]$  degrees for the angle of attack. The set of design points used in the function fits contain points relatively close to the original points and points at the boundary.

The drag coefficient on the wing at the original design point is 0.012630. The lift coefficient & pitching moment (on the wing) are 0.44397 and  $-0.14365$  respectively.

The aim of the optimisation is always to improve the design when compared with the wing performance at the initial chosen design point.

The objective in the single-point optimisations is to minimise the drag over the wing whilst retaining the lift, and not permitting the pitching moment to reduce. It is also important to ensure that constraints are added to the fuselage to maintain the lift and prevent the drag from increasing and the pitching moment from decreasing. Other requirements are to maintain the planform area, to prevent the drag over the whole configuration from increasing and to weaken the shocks on the wing surface.

Many optimisers increase the rear wing loading when attempting to weaken the wing shock, so this tendency must be avoided through the use of further constraints on the surface Mach number and the surface pressure. This increases the number of constraints by up to another 10 for the wing surfaces and up to another 20 for the fuselage surfaces from the multi-block mesh.

In the multi-point problems three points in design space with different angles of attack are used. The objective function is a weighted combination of the drag coefficients at these points. The same types of constraints as in the single point optimisation are then applied at the three points.

#### Time savings

The run-time saved by using the perturbation code where possible during the data gathering and optimisation procedures is between 75% - 86% in using approach 2 compared with approach 1, and 82%-87% for approach 4 compared with approach 3.

The CFD runs use a previous converged flow field as starting data (when appropriate) and are run until changes between iterations in the density and velocity are less than  $10^{-3}$ . The inaccuracies from the perturbation code do not cause the optimisation to take greatly different vectors through the design space during the line search process, or to invoke more iterations before convergence. As expected approach 3, where all the data are from the CFD code and no function-fits or perturbation data are used, is the most expensive approach.

In approach 2 the cost of solving the problem, including running the CFD code on the predicted design point is equivalent to 7 CFD runs for cases where the function fitting is adequate. If the design space needs to be shrunk and the optimisation re-run, and then the prediction point checked by CFD, the further cost is 3 CFD runs.

#### Single point design improvements

The following results are from approaches 1 & 2. The optimised solutions are in agreement with those found using approaches 3 & 4.

Inequality constraints on the lift and the pitching moment allow the lift to increase by a few percent above the original value whilst the pitching moment is prevented from decreasing.

The results from four cases are shown in Table 1. The first case (10 design variables) has the twist, angle of attack and camber varying, excepting the root camber, which is fixed at zero. Case 2 permits the root camber to vary as well. Cases 3 & 4 also have the position of maximum thickness varying. Case 3, the 15 variable case, does not allow the root camber to vary, whereas case 4 does (i.e. 16 design variables).

Comparing the values from the function fits with the corresponding CFD values on the optimised geometries shows an error of up to 1.9% for the drag and 0.3% for the lift and pitching moment.

For example, for the 16 design variable case, the percentage reduction in the coefficient of drag on the optimised wing compared with that on the original wing is 7.7% with  $C_D=0.011657$ . (The values compared are from the CFD code on the original and optimised geometries.) Considering both the wing and fuselage sections, total lift is maintained, the drag coefficient reduces by 5.5% and the pitching moment increases by 2%.

The change to the design variables is to introduce camber (negative) into the wing sections (except for the root section, which is fixed at zero) causing the tail to rise slightly. The position of maximum thickness moves forward to 0.25 at all but the crank section, where it moves back to 0.426. The twist vector is now (1.09, 2.44, -0.17, -0.56, -1.40) whereas the angle of attack is relatively unaffected by the optimisation and changes to 0.47 degrees. The variation in shape is shown in Figure 10 at the crank and the tip.

The  $C_p$  distribution on the upper wing for the optimised solution from the 15 variable case is shown in Figure 11. Also shown are sectional cuts at 10%, 40% and 75% of the wingspan. Compared with the original the optimised distributions show no increase in wing loading to the rear of the aerofoil, but there is in-board loading. There is a small change in the position of the shock near the trailing edge and a slight reduction in its strength. On the 10% and 40% diagrams, there is a small shock in the middle of the upper surface. In the optimised case this shock has moved in the trailing edge direction with a definite reduction in strength. This movement is due to the shift in the position of maximum thickness.

The preferred  $C_p$  distribution is a continuing decrease along the upper surface, indicating that supersonic flow is decelerated along the surface. The non-monotonic  $C_p$  distributions at the 10% and 40% wingspan positions show that there is room for further improvement in the design. Locating solutions in design space with a smooth, monotonic distribution requires adding extra constraints (after, say, 10% chord) on the pressure gradient. This information is also stored by the perturbation code.

In the cases where the position of maximum thickness is kept fixed at the original value in each section, there the maximum Mach numbers on the upper and lower surfaces reduce slightly. If the position of maximum thickness is allowed to vary in the optimisation, the drag reduction is higher, but the maximum Mach number increases. On the lower surface, this rises from M1.07 on the original geometry to M1.5 on the optimised geometry. On the upper surface there is a slight reduction from M1.39 on the original to M1.37 on the optimised wing. By setting constraints on the surface Mach number, the shock strengths can be prevented from increasing. The surface Mach numbers evaluated when the forces and moments coefficients were calculated are function fitted and added to the problem as inequality constraints.

If the constraints are set on the wing surfaces such that their value cannot be larger than the original maximum surface Mach numbers, the drag coefficient becomes 0.012407, a reduction from the original value of 2%. The wing shape lies between that of the original and the

Design variables		% reduction in $C_D$	% increase in $C_L$	% increase in $C_M$
10	4 camber, 5 twist, $\alpha$	2.1	0.0	0.7
11	5 camber, 5 twist, $\alpha$	5.1	0.0	0.7
15	4 camber, 5 twist, $\alpha$ , 5 PosMaxT	3.1	1.0	0.0
16	5 camber, 5 twist, $\alpha$ , 5 PosMaxT	7.7	0.4	0.7

Table 1 Percentage reduction in drag for the optimisation cases compared with the values on the original wing. The number of design variables perturbed varies from 10 to 16.

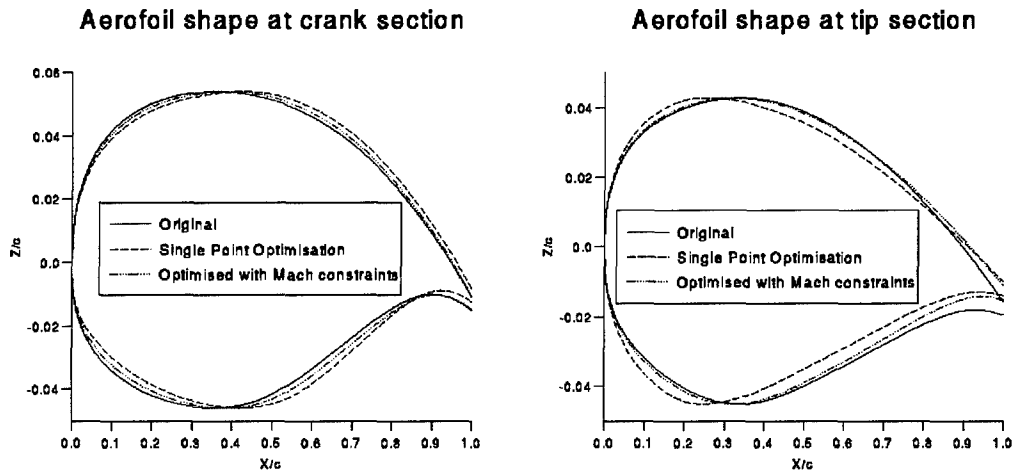


Figure 10 Wing sections at the crank and the tip. Comparison is made between the original, the optimised result without surface constraints and the result from optimising with surface constraints on the wing.

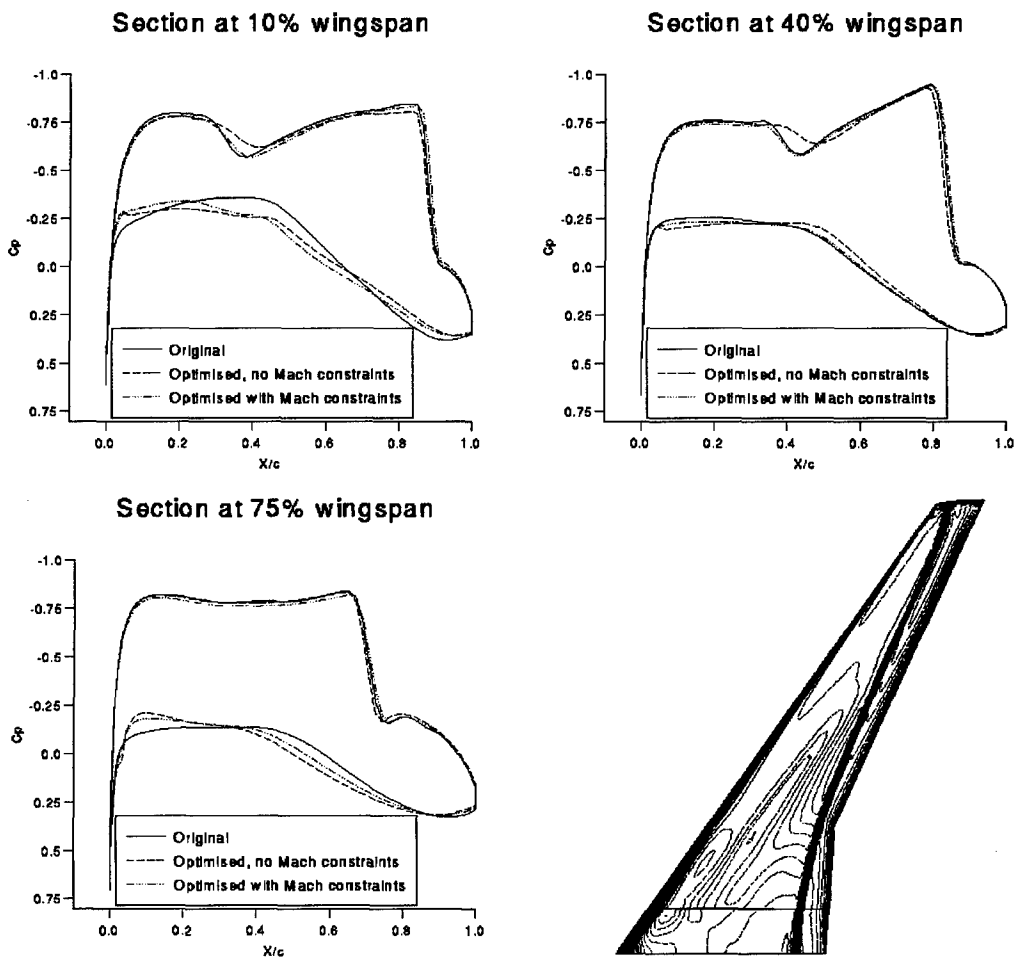


Figure 11.  $C_p$  distributions at 10%, 40% and 75% of the wingspan. On each graph are displayed the  $C_p$  distribution on the original and optimized wings including the  $C_p$  distribution from the case where constraints are applied to the surface Mach number. Also shown is the  $C_p$  distribution on the upper surface of the optimized wing.



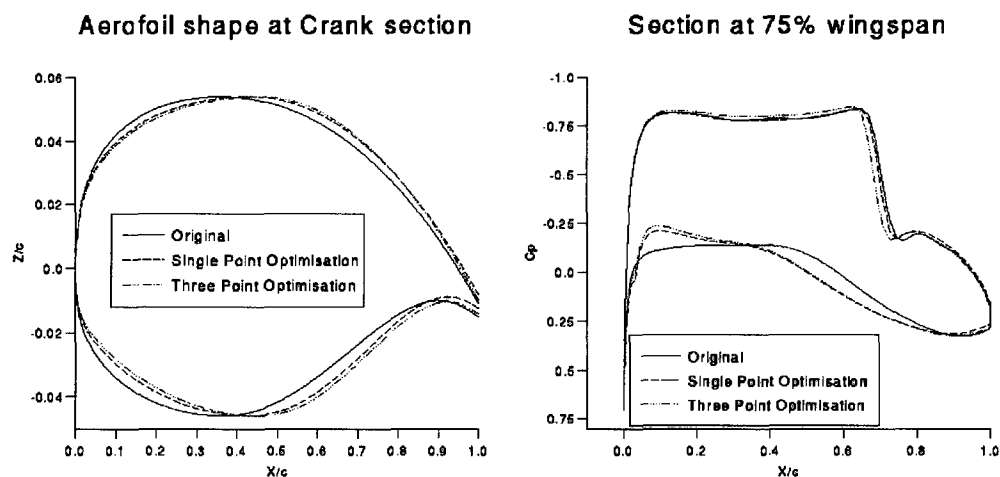


Figure 12. Results from the 3-point optimization run. On the left hand diagram comparison is made between the aerofoil sections at the crank for the original, single point and three point cases. On the right hand diagram comparisons are shown of the  $C_p$  distributions at 75% of the wingspan for the three cases.

optimised (without Mach constraints) shape (see Figure 10). The angle of attack drops to 0.37 degrees.

#### Design improvements through multi-point optimisation

In this investigation of off-design conditions, three points are chosen for their wing lift coefficient values of 0.44397, 0.4 and 0.37. On the original wing-body configuration, these correspond to angles of attack at 0.5, 0.21 and 0.0 degrees. Hence the problem has 18 design variables: fifteen shape (i.e. camber, twist and position of maximum thickness) and 3 angles of attack. Constraints are set on the lift coefficients to maintain the same lift as on the original wing and the pitching moments to ensure that they do not become more negative. The objective function is a weighted sum of the drag coefficient values at each of the three angles of attack.

The first case shown is where equal weighting has been adopted, the second case is where 90% weighting is on the point with lowest  $C_L$  and 5% each on the points with larger  $C_L$ . The third case has 90% weighting on the point with highest  $C_L$  and 5% each on the other points.

In this type of case, approach 2 can save between 75%-86% of the time required by approach 1, and approach 4 is 84%-89% cheaper than approach 3.

Table 2 lists the change in the angle of attack from the original values for the case with equal weighting. The change to the shape of the wing is in keeping with the single point result: the introduction of camber, small changes in twist and a shift in the positions of maximum thickness in each wing section (see Figure 12).

$C_L$	Angle of attack (degrees)	
	Original	Optimised
0.44397	0.5	0.690
0.4	0.21	0.408
0.37	0.0	0.204

Table 2: Change in angle of attack in the three-point optimisation case with equal weighting.

The combined drag reductions for the equal and unequal weighted cases are shown in Table 3. The equal-weighted case is less successful in reducing the combined drag than cases where the weighting is unequal.

The  $C_p$  distribution on the optimised wing at 75% wingspan is shown in Figure 12. The results of the three point optimisation enhance the trends seen with the single point optimisation with the shock position being moved forward slightly.

	Combined $C_D$	
	Original	Optimised
Weighting		
Case 1 (0.33,0.33,0.33)	0.010219	0.009423
Case2 (0.05,0.05,0.9)	0.008658	0.007074
Case3 (0.9,0.05,0.05)	0.012108	0.010525

Table 3: Change in the combined  $C_D$  due to different weightings. Values on the original & optimised aerofoils.

#### Conclusions

Approximation methods can be valuable tools in design improvement studies. Careful use can reduce the time to find suitable solutions to design problems by up to 90% compared with using the very accurate CFD codes for production of all required data. If due care is taken, methods of varying accuracy, e.g. perturbation methods, CFD and function fitting algorithms can be complementary in proving the optimiser with good quality, useful data.

The development of a perturbation code can be a valuable aid in design studies, particularly in the evaluation of gradients, rapid production of data and as an exploration tool over a small region of design space.

Function fitting data rapidly reduces the cost of optimisation cases as long as the response surfaces are good representative views of the design space. To reach this stage, the function fits may need to be improved in a number of optimisation runs. This enables regions of

interest to be identified, new data evaluated and function fits of each local area improved.

The frameworks used to find design improvement configurations need to be easily modified as knowledge is built up about the design space considered. The response surface functions should be easily amenable to include more design parameters. Constraint functions may need to be amended or new constraints added in an attempt to enhance or remove certain features in the results.

To produce design improvements that are of practical use, multi-point studies are important. This prevents designs being considered in which small changes in flight conditions produce large changes in the vehicle's performance.

Although the results presented here are for Euler flows, the aim of the research is to use the design improvement approach(es) as the first of two stages. The second stage uses the Euler predictions of which design points are of interest but includes viscous flow predictions. In this way considerable time can be saved compared to evaluating all data for the optimisation studies from Navier-Stokes CFD codes.

#### **Acknowledgements**

This work was funded jointly by the Royal Academy of Engineering, London, U.K. and British Aerospace's Sowerby Research Centre.

#### **References**

- [1]- Aerodynamic Optimisation using Analytic Descriptions of the Design Space.  
C. A. Toomer, M. E. Topliss & D. P. Hills.  
AIAA-96-4141 and 6th AIAA/NASA/USAF Multi-disciplinary Analysis & Optimization Symposium, Bellevue, WA., Sept. 1996
- [2]- Research of Projected Implicit Reconstruction in Optimisation. A. J. A. van Etten. Report No. WFW 96.063, Eindhoven University of Technology, May 1996.
- [3]- MDO process and Specification for the Primary Sensitivities Study. Industrial & Materials Technology Programme. S. Allwright. British Aerospace PLC.  
April 1996
- [4]- MULTI-BLOCK Navier-Stokes solver RANSMB user guide. J. J. Benton. British Aerospace internal report ADE-ETA-R-FM-0121. 1993
- [5]- Rapid Design Space Approximations for a Two-Dimensional Transonic Aerofoil.  
M. E. Topliss, C. A. Toomer & D. P. Hills. AIAA-96-0095 and AIAA Journal of Aircraft, Vol. 33, No. 6 Nov.-Dec. 1996, pp 1101-1108.
- [6]- E04UCF. NAG Fortran library Mark 16. NAG Ltd., 1993.